Beyond 100 Gb/s Optical Transmission Based on Polarization Multiplexed Coded-OFDM With Coherent Detection

Ivan B. Djordjevic, Lei Xu, and Ting Wang

***Abstract*—We propose a coded-modulation scheme suitable for beyond 100 Gb/s transmission and 100 Gb/s Ethernet. It is based on polarization multiplexed coded-orthogonal frequency division multiplexing (OFDM). By using 32-QAM-based polarization multiplexed coded-OFDM, we are able to achieve the aggregate rate of 100 Gb/s, while the OFDM signal bandwidth is only 10 GHz, resulting in a spectral efficiency of 10 bits/s/Hz. The spectral efficiency of the proposed scheme is twice higher than that of the polarization diversity OFDM scheme. We show that the proposed multicarrier scheme is insensitive to polarization mode dispersion (PMD), while the PMD represents a major source of performance degradation in single carrier systems, in addition to fiber nonlinearities. We also describe how to determine the symbols' log-likelihood ratios in the presence of laser phase noise.**

***Index Terms*—Optical communications; Polarization mode dispersion (PMD); Low-density parity-check (LDPC) codes; Polarization diversity; Polarization multiplexing; Orthogonal frequency division multiplexing (OFDM); 100 Gb/s Ethernet**.

I. Introduction

Optical communication systems are developing rapidly due to the increased demands on transmission capacity. Network operators already consider 100 Gb/s per dense wavelength division multiplexing (DWDM) channel transmission. However, the performance of fiber-optic communication systems operating at those data rates is degraded significantly due to several transmission impairments including intra- and inter-channel nonlinearities, polarization mode dispersion (PMD), and chromatic dispersion [1–14]. To deal with chromatic dispersion and PMD a number of channel equalization techniques have been proposed recently, including a digital filtering approach [11,12], maximum likelihood sequence detection (MLSD) [4,9], and turbo equalization [2,8]. To simultaneously suppress chromatic dispersion and PMD, orthogonal frequency division multiplexing (OFDM) has been advocated [5–7,10]. To deal with intra-channel nonlinearities someone may use either constrained coding [3] or turbo equalization [8].

In this paper we propose a coded-modulation scheme suitable for beyond 100 Gb/s optical transmission based on coded-OFDM and polarization multiplexing. By using 32-QAM polarization multiplexed coded-OFDM we are able to achieve the aggregate data rate of 100 Gb/s for OFDM signal bandwidth of only 10 GHz, resulting in a spectral efficiency of 10 bits/s/Hz. The tolerance to PMD of the proposed scheme is comparable to the corresponding polarization diversity scheme, but offers two times higher spectral efficiency. (Notice that we use the term diversity in the same fashion that is used in wireless communications [15,16], which is different from the polarization multiplexing [11], and denotes that the same symbol is transmitted using both polarizations.) While the PMD in single carrier systems at high speeds represents a major performance degradation factor (in addition to Kerr nonlinearities), the penalty due to PMD in the proposed coded-modulation scheme is negligible.

The arbitrary forward error correction (FEC) scheme can be used with the proposed polarization multiplexed coded-OFDM scheme. However, the use of large-girth low-density parity-check (LDPC) codes [14] leads to the channel capacity achieving performance. We also describe how to determine the symbols' reliabilities (i.e., the symbol log-likelihood ratios) in the presence of laser phase noise.

II. Description of the Proposed Polarization Multiplexed Coded-OFDM Scheme

It has been shown by Shieh *et al.* in [5–7] that the polarization diversity OFDM is able to compensate

Manuscript received October 19, 2008; accepted December 29, 2008; published June 1, 2009 (Doc. ID 110471).

I. B. Djordjevic is with the University of Arizona, Department of Electrical and Computer Engineering, Tucson, AZ 85721, USA (e-mail: ivan@ece.arizona.edu).

L. Xu and T. Wang are with NEC Laboratories America, Princeton, NJ 08540, USA.

Digital Object Identifier 10.1364/JOCN.1.000050

all-order PMD with small penalties. Moreover, the PMD improves the system margin for PDL-induced penalty [7]. Therefore, for evaluation of different OFDM schemes it is sufficient to observe the first-order PMD. For the first-order PMD study the Jones matrix, neglecting the polarization-dependent loss and depolarization effects due to nonlinearity, can be represented in a fashion similar to [13] by

$$H(\omega)=\begin{bmatrix} h_{xx}(\omega) & h_{xy}(\omega) \\ h_{yx}(\omega) & h_{yy}(\omega) \end{bmatrix}=R^{-1}P(\omega)R,$$

$$P(\omega)=\begin{bmatrix} e^{-j\omega\tau/2} & 0 \\ 0 & e^{j\omega\tau/2} \end{bmatrix}, \quad (1)$$

where τ denotes DGD, $R=R(\theta,\varepsilon)$ is the rotational matrix defined by

$$R=\begin{bmatrix} \cos(\theta/2)e^{j\varepsilon/2} & \sin(\theta/2)e^{-j\varepsilon/2} \\ -\sin(\theta/2)e^{j\varepsilon/2} & \cos(\theta/2)e^{-j\varepsilon/2} \end{bmatrix}, \quad (2)$$

θ denotes the polar angle, ε denotes the azimuth angle, and ω is the angular frequency. For coherent detection OFDM, the received symbol vector $r_{i,k}=[r_{x,i,k}r_{y,i,k}]^T$ at the ith OFDM symbol and kth subcarrier can be represented by

$$r_{i,k}=H(k)s_{i,k}e^{j\phi_{PN}}+n_{i,k}, \quad (3)$$

where $s_{i,k}=[s_{x,i,k}s_{y,i,k}]^T$ denotes the transmitted symbol vector, $n_{i,k}=[n_{x,i,k}n_{y,i,k}]^T$ denotes the noise vector due to the amplified spontaneous emission (ASE), and the Jones matrix H was introduced in Eq. (1). Here we use index k to denote the kth subcarrier frequency ω_k. ϕ_{PN} denotes the phase noise process $\phi_{PN}=\phi_T-\phi_{LO}$ due to the laser phase noise processes of transmitting laser ϕ_T and local laser ϕ_{LO} that are commonly modeled as the Wiener–Lévy processes [17], which are zero-mean Gaussian processes with corresponding variances being $2\pi\Delta\nu_T|t|$ and $2\pi\Delta\nu_{LO}|t|$, where $\Delta\nu_T$ and $\Delta\nu_{LO}$ are the laser linewidths of the transmitting and receiving laser, respectively. The transmitted/received symbols per subcarrier are complex-valued, with the real part corresponding to the in-phase coordinate and the imaginary part corresponding to the quadrature coordinate of a corresponding signal constellation point. Figure 1 shows the magnitude responses of the h_{xx} and h_{xy} coefficients of the Jones matrix against the normalized frequency $f\tau$ (the frequency here is normalized with DGD τ so that the conclusions are independent on the bit rate) for two different cases: (a) $\theta=\pi/2$ and $\varepsilon=0$, and (b) $\theta=\pi/3$ and $\varepsilon=0$. In the first case channel coefficient h_{xx} tends to zero for certain frequencies, while in the second case it never becomes zero, suggesting that the first case represents the worst case scenario, and as such is considered in Section III.

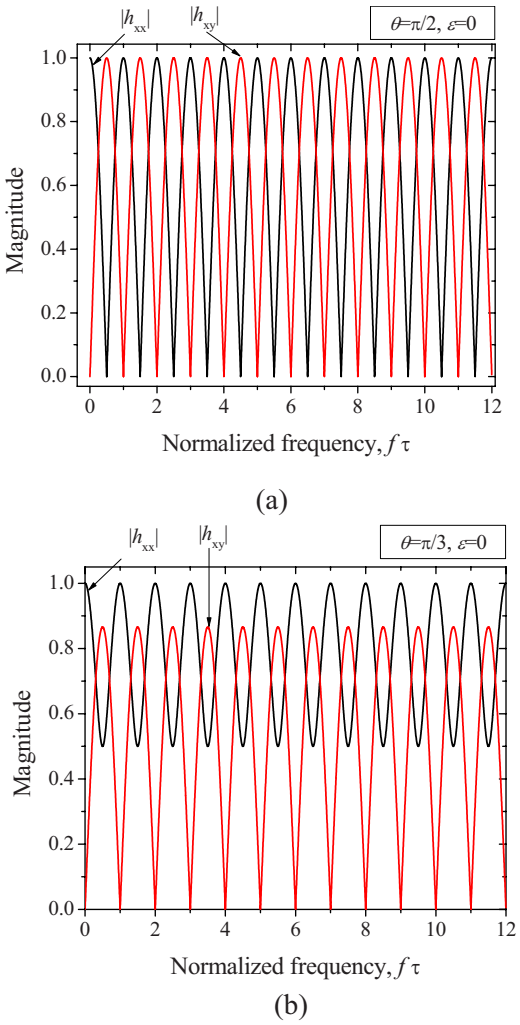

Fig. 1. (Color online) Magnitude response of h_{xx} and h_{xy} Jones matrix coefficients against the normalized frequency for (a) $\theta=\pi/2$ and $\varepsilon=0$, and (b) $\theta=\pi/3$ and $\varepsilon=0$.

The proposed coded-OFDM scheme, with an LDPC code as the channel code, is shown in Fig. 2. The bit streams originating from m different information sources are encoded using different (n,k_i) LDPC codes of code rate $r_i=k_i/n$. k_i denotes the number of information bits of the ith $(i=1,2,\ldots,m)$ component LDPC code, and n denotes the codeword length, which is the same for all LDPC codes. The use of different LDPC codes allows us to optimally allocate the code rates. If all component LDPC codes are identical, the corresponding scheme is commonly referred to as the bit-interleaved coded modulation (BICM). The outputs of m LDPC encoders are written row-wise into a block-interleaver block. The mapper accepts m bits at time instance i from the $(m\times n)$ interleaver column-wise and determines the corresponding M-ary $(M=2^m)$ signal constellation point $(\phi_{I,i},\phi_{Q,i})$ in a two-dimensional (2D) constellation diagram such as M-ary PSK or M-ary QAM. (The coordinates correspond to in-phase and quadrature components of M-ary 2D constellation.) The OFDM symbol is generated as described be-

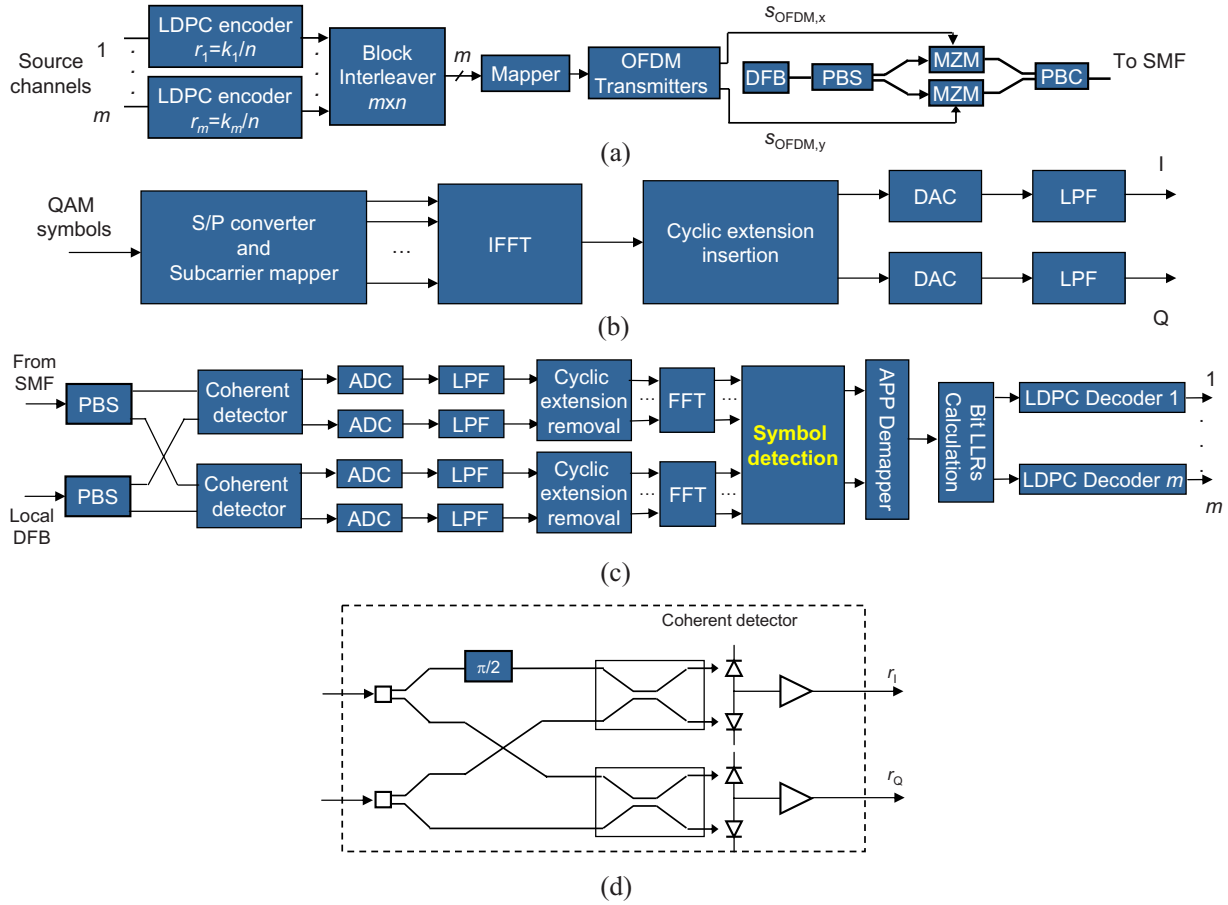

Fig. 2. (Color online) The architecture of the polarization-multiplexed LDPC-coded OFDM scheme: (a) transmitter architecture, (b) OFDM transmitter architecture (*x*- or *y*-polarization), (c) receiver architecture, and (d) balanced coherent detector configuration. DFB, distributed feedback laser; PBS(C), polarization beam splitter (combiner); MZM, dual-drive Mach–Zehnder modulator; APP, a posteriory probability; LLRs, log-likelihood ratios.

low. N_{QAM} input QAM symbols are zero-padded to obtain N_{FFT} input samples for inverse FFT (IFFT) (the zeros are inserted in the middle rather than at the edges), and N_G non-zero samples are inserted to create the guard interval. For efficient chromatic dispersion and PMD compensation, the length of the cyclically extended guard interval should be longer than the total spread due to chromatic dispersion and the maximum value of DGD. The cyclic extension is obtained by repeating the last $N_G/2$ samples of the effective OFDM symbol part (N_{FFT} samples) as a prefix and repeating the first $N_G/2$ samples as a suffix. After D/A conversion (DAC), the OFDM signal is converted into the optical domain using the dual-drive Mach–Zehnder modulator (MZM). Two MZMs are needed, one for each polarization. The outputs of MZMs are combined using the polarization beam combiner (PBC). The same DFB laser is used as a CW source, with *x*- and *y*-polarization being separated by a polarization beam splitter (PBS). Given the fact that the complexity of the MLC scheme is high for high speed implementation, the BICM is adopted in the rest of the paper.

The 100 Gb/s aggregate data rate can be achieved as follows. By setting the OFDM signal bandwidth to 10 GHz and by employing the polarization multiplexing and 32-QAM we can achieve 100 Gb/s, with a spectral efficiency of 10 bits/s/Hz. Another option would be to use 16-QAM, but setting the OFDM signal bandwidth to 12.5 GHz. However, the spectral efficiency would be smaller (8 bits/s/Hz). Both options employ mature 10 Gb/s technology while achieving the aggregate rate of 100 Gb/s. The operations of all blocks, except the symbol detector shown in Fig. 2(c), are similar to those we reported in [1,10], and for more details on OFDM with coherent detection an interested reader is referred to an excellent tutorial paper due to Shieh *et al.* [7]. Here we describe the operation of the symbol detector block, the calculation of symbol log-likelihood ratios (LLRs), and the calculation of bit LLRs, in the presence of laser phase noise. By re-writing Eq. (3) in scalar form we obtain, by ignoring the laser phase noise at the moment to keep the explanation simpler,

$$r_{x,i,k} = h_{xx}(k)s_{x,i,k} + h_{xy}(k)s_{y,i,k} + n_{x,i,k}, \qquad (4)$$

$$r_{y,i,k} = h_{yx}(k)s_{x,i,k} + h_{yy}(k)s_{y,i,k} + n_{y,i,k}, \tag{5}$$

where index k denotes the kth subcarrier, index i denotes the ith OFDM symbol, $h_{ij}(k)(i,j \in \{x,y\})$ are the channel coefficients due to PMD introduced by Eq. (1), $s_{x,i,k}$ and $s_{y,i,k}$ denote the transmitted symbols in x- and y-polarization, respectively, and corresponding received symbols are denoted by $r_{x,i,k}$ and $r_{y,i,k}$. In Eqs. (4) and (5) $n_{x,i,k}$ and $n_{y,i,k}$ denote the ASE noise processes in x- and y-polarization. The equivalent channel model is shown in Fig. 3, and it is consistent with previous literature [6,7]. In the absence of ASE noise, Eqs. (4) and (5) represent the system of linear equations with two unknowns $s_{x,i,k}$ and $s_{y,i,k}$. By multiplying Eq. (4) with $h_{xx}(k)/|h_{xx}(k)|^2$ and Eq. (5) with $h_{yy}(k)/|h_{yy}(k)|^2$, the unknown transmitted symbols can be estimated by

$$s'_{x,i,k} = \frac{\dfrac{h^*_{xx}(k)}{|h_{xx}(k)|^2}\left[r_{x,i,k} - \dfrac{h_{xy}(k)h^*_{yy}(k)}{|h_{yy}(k)|^2}r_{y,i,k}\right]}{1 - \dfrac{h^*_{xx}(k)h_{xy}(k)}{|h_{xx}(k)|^2}\dfrac{h_{yx}(k)h^*_{yy}(k)}{|h_{yy}(k)|^2}}, \tag{6}$$

$$s'_{y,i,k} = \frac{h^*_{yy}(k)}{|h_{yy}(k)|^2}r_{y,i,k} - \frac{h_{yx}(k)h^*_{yy}(k)}{|h_{yy}(k)|^2}s'_{x,i,k}, \tag{7}$$

where $s'_{x,i,k}$ and $s'_{y,i,k}$ denote the detector estimates of symbols $s_{x,i,k}$ and $s_{y,i,k}$ transmitted on the kth subcarrier of the ith OFDM symbol. Notice that the OFDM scheme with polarization diversity [7], assuming that both polarizations are used on a transmitter side and equal-gain combining on a receiver side, is the special case of the symbol detector described by Eqs. (6) and (7). By setting $s_{x,i,k}=s_{y,i,k}=s_{i,k}$ and using the symmetry of channel coefficients, the transmitted symbol can be estimated by

$$s'_{i,k} = (h^*_{xx}(k)r_{x,i,k} + h^*_{xy}(k)r_{y,i,k})/(|h_{xx}(k)|^2 + |h_{xy}(k)|^2).$$

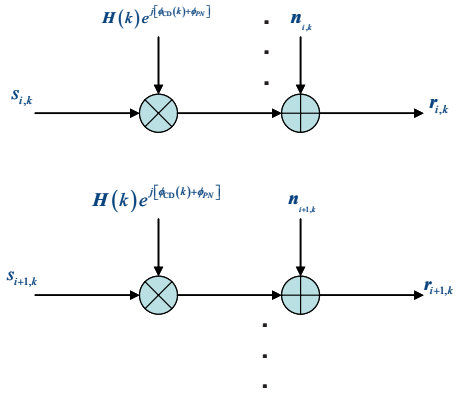

Fig. 3. (Color online) Equivalent OFDM channel model. $\phi_{CD}(k)$ denotes the phase distortion of the kth subcarrier due to chromatic dispersion.

In the presence of laser phase noise the symbol detector estimates are a function of the laser phase noise process:

$$s'_{x,i,k} = \frac{\dfrac{h^*_{xx}(k)e^{-j\phi_{PN}}}{|h_{xx}(k)|^2}\left[r_{x,i,k} - \dfrac{h_{xy}(k)h^*_{yy}(k)}{|h_{yy}(k)|^2}r_{y,i,k}\right]}{1 - \dfrac{h^*_{xx}(k)h_{xy}(k)}{|h_{xx}(k)|^2}\dfrac{h_{yx}(k)h^*_{yy}(k)}{|h_{yy}(k)|^2}}, \tag{8}$$

$$s'_{y,i,k} = \frac{h^*_{yy}(k)e^{-j\phi_{PN}}}{|h_{yy}(k)|^2}r_{y,i,k} - \frac{h_{yx}(k)h^*_{yy}(k)}{|h_{yy}(k)|^2}s'_{x,i,k}. \tag{9}$$

The detector soft estimates of symbols carried by the kth subcarrier in the ith OFDM symbol, $s'_{x(y),i,k}$, are forwarded to the *a posteriori* probability (APP) demapper, which determines the symbol LLRs $\lambda_{x(y)}(s)$ of x- (y-) polarization by

$$\lambda_{x(y)}(s|\phi_{PN}) = -\frac{(\Re[s'_{x(y),i,k}(\phi_{PN})] - \Re[\mathrm{QAM}(\mathrm{map}(s))])^2}{2\sigma^2} - \frac{(\Im[s'_{x(y),i,k}(\phi_{PN})] - \Im[\mathrm{QAM}(\mathrm{map}(s))])^2}{2\sigma^2};$$

$$s = 0,1,\ldots,2^{n_b}-1 \tag{10}$$

where $\Re[]$ and $\Im[]$ denote the real and imaginary parts of a complex number, QAM denotes the QAM-constellation diagram, σ^2 denotes the variance of an equivalent Gaussian noise process originating from ASE noise, and map(s) denotes a corresponding mapping rule (Gray mapping rule is applied here). (n_b denotes the number of bits carried by the symbol.) Notice that symbol LLRs in Eq. (10) are conditioned on the laser phase noise sample $\phi_{PN}=\phi_T-\phi_{LO}$, which is a zero-mean Gaussian process (the Wiener–Lévy process [17]) with a variance of $\sigma^2_{PN}=2\pi(\Delta\nu_T+\Delta\nu_{LO})|t|$ ($\Delta\nu_T$ and $\Delta\nu_{LO}$ are the corresponding laser linewidths introduced earlier). This comes from the fact that estimated symbols $s'_{x(y),i,k}$ are functions of ϕ_{PN}. To remove the dependence on ϕ_{PN} we have to average the likelihood function (not its logarithm), over all possible values of ϕ_{PN}:

$$\lambda_{x(y)}(s) = \log\int_{-\infty}^{\infty} e^{\lambda_{x(y)}(s|\phi_{PN})}\frac{1}{\sigma_{PN}\sqrt{2\pi}}e^{-\phi^2_{PN}/2\sigma^2_{PN}}d\phi_{PN}. \tag{11}$$

The calculation of LLRs in Eq. (11) can be performed by numerical integration. For the laser linewidths considered in this paper it is sufficient to use the trapezoidal rule, with samples of ϕ_{PN} obtained by pilot-aided channel estimation as explained in [6].

Let us denote by $b_{j,x(y)}$ the jth bit in an observed symbol s binary representation $b=(b_1,b_2,\ldots,b_{n_b})$ for x- (y-) polarization. The bit LLRs required for LDPC decoding are calculated from symbol LLRs by

$$L(b'_{j,x(y)}) = \log \frac{\sum_{s:b_j=0} \exp\{\lambda_{x(y)}(s)\}}{\sum_{s:b_j=1} \exp\{\lambda_{x(y)}(s)\}}. \quad (12)$$

The jth bit LLR in Eq. (12) is calculated as the logarithm of the ratio of a probability that $b_j=0$ and probability that $b_j=1$. In the numerator, the summation is done over all symbols s having 0 at the position j. Similarly, in the denominator summation is performed over all symbols s having 1 at the position j.

The bit LLRs calculated by Eq. (12) are forwarded to the corresponding LDPC decoders, as shown in Fig. 2(c). The LDPC decoders from Fig. 2(c) employ the sum-product-with-correction term algorithm. The LDPC code used in this paper belongs to the class of quasi-cyclic (array) codes of large girth ($g \geq 10$) [14], so that the corresponding decoder complexity is low compared to random LDPC codes, and does not exhibit the error floor phenomenon in the region of interest in fiber-optics communications ($\leq 10^{-15}$).

III. Evaluation of the Proposed Coded-Modulation Scheme in the Presence of PMD

We are turning our attention to the evaluation of the proposed scheme. To illustrate the efficiency of this scheme, in Fig. 4 we show the constellation diagrams for an aggregate rate of 100 Gb/s, corresponding to the $M=32$ QAM and the OFDM signal bandwidth of 10 GHz, before [see Fig. 4(a)] and after [see Fig. 4(b)] PMD compensation, assuming the worst-case scenario ($\theta=\pi/2, \varepsilon=0$). The symbol detection scheme described above is able to completely compensate the first-order PMD with DGD of even 1200 ps. In Fig. 5 we show both the uncoded and LDPC-coded BER performance of the proposed scheme against the polarization diversity OFDM scheme with coherent detection, for different constellations sizes. The component LDPC code is based on the girth-10 LDPC(16935,13550) code. For $M=4$ QAM (QPSK), the OFDM system parameters were chosen as follows: the number of QAM symbols $N_{QAM}=512$, the oversampling is two times, OFDM signal bandwidth is set to 10 GHz, and the number of samples used in cyclic extension is $N_G=16$. For other constellation sizes ($M=16,32,64$), the OFDM system parameters were chosen as follows: the number of QAM symbols $N_{QAM}=2048$, the oversampling is two times, OFDM signal bandwidth is set to 10 GHz, and the number of samples used in cyclic extension is $N_G=64$. In simulations, for the polarization diversity OFDM scheme,

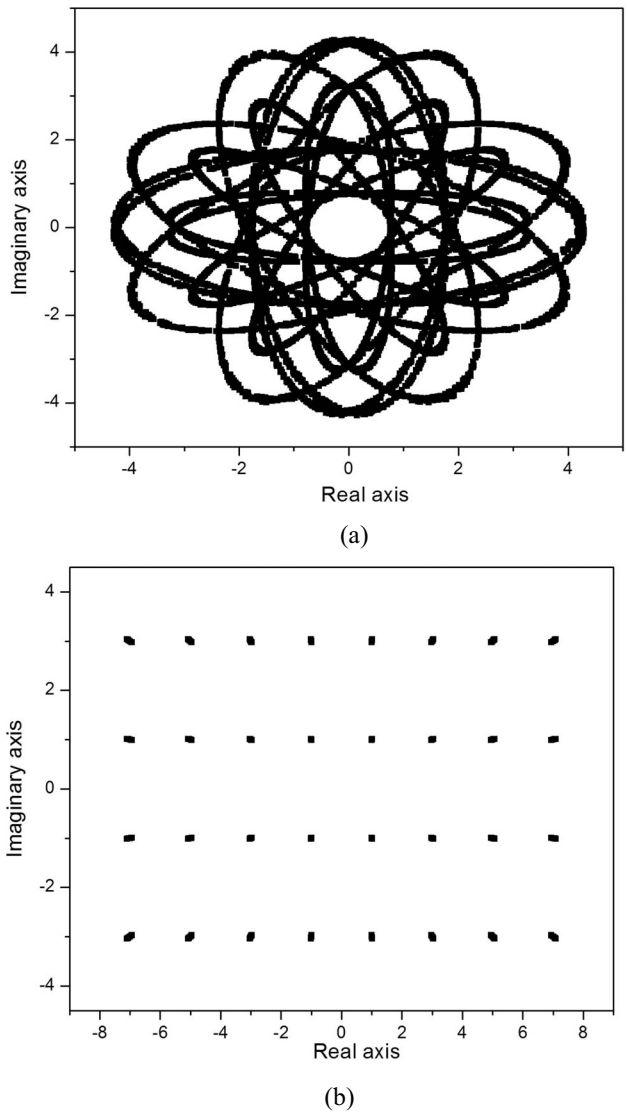

Fig. 4. The constellation diagrams for $M=32$ QAM (the aggregate data rate is 100 Gb/s) after 1200 ps of DGD observing the worst-case scenario ($\theta=\pi/2$, $\varepsilon=0$) (a) before PMD compensation and (b) after PMD compensation.

the same OFDM signal was transmitted over both polarizations. For the fair comparison of different M-ary schemes the OSNR on the x-axis is given per information bit, which is also consistent with the digital communication literature [15,16]. The code rate influence is included in Fig. 5 so that the corresponding coding gains are net effective coding gains. The average launch power per OFDM symbol is set to −3 dBm (and similarly as in wireless communications [15,16] represents the power per information symbol), and the Gray mapping rule is employed.

For DGD of 1200 ps, the proposed scheme performs comparable to the polarization-diversity OFDM in terms of BER (the corresponding curves overlap each other), but has two times higher spectral efficiency. For example, the aggregate data rate for $M=32$ QAM and polarization multiplexed coded-OFDM is

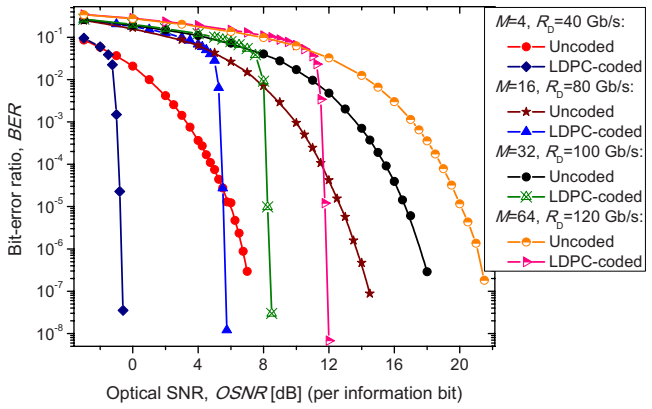

Fig. 5. (Color online) BER performance of the proposed polarization multiplexed coded-OFDM scheme, for DGD of 1200 ps and the worst-case scenario ($\theta=\pi/2$, $\varepsilon=0$). R_D denotes the aggregate data rate.

100 Gb/s, while the aggregate rate of polarization diversity coded-OFDM scheme is 50 Gb/s.

The aggregate data rate of 100 Gb/s can also be achieved for single carrier systems based on 32-QAM and polarization diversity. However, to deal with PMD someone has to use maximum-likelihood sequence detection (MLSD) [4,9], turbo equalization [2,8], or the digital filtering approach [11]. The detector complexity of the corresponding turbo equalization or MLSD schemes grows exponentially as DGD increases [mostly due to the complexity of the Bahl–Cocke–Jelinek–Raviv (BCJR) and Viterbi algorithms [2,8], and for DGD of 1200 ps it would require the trellis description (see [2,8]) with too many states to be of practical importance. The proposed scheme also outperforms the scheme implemented by Nortel Networks researchers [11], capable of compensating the rapidly varying first order PMD with peak DGD of 150 ps [11]. The receiver complexity of polarization multiplexed coded-OFDM is comparable to that of the coded-OFDM with polarization diversity. The net effective coding gain increases as the constellation size grows. For $M=4$ QAM based polarization multiplexed coded-OFDM the net effective coding gain is 8.36 dB at BER of 10^{-7}, while for $M=32$ QAM based LPDC-coded OFDM (of aggregate data rate 100 Gb/s) the coding gain is 9.53 dB at the same BER. The larger net effective coding gains are expected at lower BERs. The laser linewidths of the transmitting and local laser were set to 10 kHz, so that the PMD and ASE noise are predominant effects. For the influence of the laser phase noise on coherent OFDM systems an interested reader is referred to [18].

IV. Conclusion

We proposed a particular polarization multiplexed coded-OFDM scheme suitable for use in beyond 100 Gb/s optical transmission and 100 Gb/s Ethernet. By selecting the OFDM signal bandwidth to be 10 GHz, and by using 32-QAM and polarization multiplexing, the aggregate data rate of 100 Gb/s is achieved. The spectral efficiency of the proposed scheme is 10 bits/s/Hz. For the same system parameters, the corresponding polarization diversity coded-OFDM would have the aggregate rate of 50 Gb/s, which is insufficient for 100 Gb/s Ethernet. Therefore, the proposed coded-modulation scheme achieves the aggregate rate of 100 Gb/s, while employing the mature 10 Gb/s technology. The proposed coded-modulation scheme is insensitive to PMD, while in corresponding single carrier systems the PMD introduces severe performance degradation. The results of simulations indicate that even 1200 ps of DGD, in polarization multiplexed coded-OFDM systems with aggregate data rate of 100 Gb/s, can completely be compensated with negligible penalty. In contrast to the PMD turbo equalization scheme whose complexity grows exponentially as DGD increases (due to the exponential increase in complexity of the BCJR algorithm [2,8]), the complexity of the proposed scheme is essentially independent on the level of DGD as long as the guard interval is longer than the maximum DGD. We also describe how to determine the symbols' log-likelihood ratios in the presence of laser phase noise.

Acknowledgment

This work is supported in part by the National Science Foundation under grant IHCS-0725405 and in part by NEC Laboratories America.

References

[1] I. B. Djordjevic, M. Cvijetic, L. Xu, and T. Wang, "Using LDPC-coded modulation and coherent detection for ultra high-speed optical transmission," *J. Lightwave Technol.*, vol. 25, pp. 3619–3625, 2007.

[2] L. L. Minkov, I. B. Djordjevic, H. G. Batshon, L. Xu, T. Wang, M. Cvijetic, and F. Kueppers, "Demonstration of PMD compensation by LDPC-coded turbo equalization and channel capacity loss characterization due to PMD and quantization," *IEEE Photon. Technol. Lett.*, vol. 19, pp. 1852–1854, 2007.

[3] I. B. Djordjevic, "Suppression of intrachannel nonlinearities in high-speed WDM systems," in *Advanced Technologies for High-Speed Optical Communications*, L. Xu, ed., p. 247–277, *Research Signpost*, 2007.

[4] N. Alic, G. C. Papen, R. E. Saperstein, R. Jiang, C. Marki, Y. Fainman, and S. Radic, "Experimental demonstration of 10 Gb/s NRZ extended dispersion-limited reach over 600 km-SMF link without optical dispersion compensation," in *Proc. OFC/NFOEC 2006*, Mar. 2006, paper OWB7.

[5] W. Shieh, W. Chen, and R. S. Tucker, "Polarization mode dispersion mitigation in coherent optical orthogonal frequency division multiplexed systems," *IEE Electron. Lett.*, vol. 42, pp. 996–997, 2006.

[6] W. Shieh, X. Yi, Y. Ma, and Y. Tang, "Theoretical and experimental study on PMD-supported transmission using polarization diversity in coherent optical OFDM systems," *Opt. Express*, vol. 15, pp. 9936–9947, 2007.

[7] W. Shieh, X. Yi, Y. Ma, and Q. Yang, "Coherent optical OFDM:

has its time come?" *J. Opt. Netw.*, vol. 7, pp. 234–255, 2008.
[8] I. B. Djordjevic, L. L. Minkov, and H. G. Batshon, "Mitigation of linear and nonlinear impairments in high-speed optical networks by using LDPC-coded turbo equalization," *IEEE J. Sel. Areas Commun.*, vol. 26, no. 6, pp. 73–83, Aug. 2008.
[9] P. Poggiolini, G. Bosco, S. Savory, Y. Benlachtar, R. I. Killey, and J. Prat, "1,040 km uncompensated IMDD transmission over G.652 fiber at 10 Gbit/s using a reduced-state SQRT-metric MLSE receiver," in *Proc. ECOC 2006*, Sept. 2006, Cannes, France, Post-Deadline Paper Th4.4.6.
[10] I. B. Djordjevic, L. Xu, and T. Wang, "Simultaneous chromatic dispersion and PMD compensation by using coded-OFDM and girth-10 LDPC codes," *Opt. Express*, vol. 16, pp. 10269–10278, 2008.
[11] H. Sun, K.-T. Wu, and K. Roberts, "Real-time measurements of a 40 Gb/s coherent system," *Opt. Express*, vol. 16, pp. 873–879, 2008.
[12] S. J. Savory, "Digital filters for coherent optical receivers," *Opt. Express*, vol. 16, pp. 804–817, 2008.
[13] D. Penninckx and V. Morenás, "Jones matrix of polarization mode dispersion," *Opt. Lett.*, vol. 24, pp. 875–877, 1999.
[14] I. B. Djordjevic, L. Xu, T. Wang, and M. Cvijetic, "Large girth low-density parity-check codes for long-haul high-speed optical communications," in *Proc. OFC/NFOEC 2008*, paper JWA53.
[15] E. Biglieri, R. Calderbank, A. Constantinides, A. Goldsmith, A. Paulraj, and H. V. Poor, *MIMO Wireless Communications*, Cambridge Univ. Press, 2007.
[16] J. G. Proakis, *Digital Communications*, Boston: McGraw-Hill, 2001.
[17] M. Cvijetic, *Coherent and Nonlinear Lightwave Communications*, Boston: Artech House, 1996.
[18] X. Yi, W. Shieh, and Y. Ma, "Phase noise effects on high spectral efficiency coherent optical OFDM transmission," *J. Lightwave Technol.*, vol. 26, pp. 1309–1316, 2008.

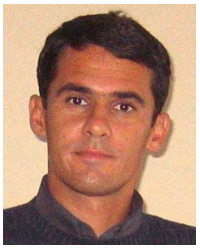

Ivan B. Djordjevic is an Assistant Professor of Electrical and Computer Engineering at the University of Arizona, Tucson. Prior to this appointment in August 2006, he was with the University of Arizona (as a Research Assistant Professor); the University of the West of England, Bristol, UK; the University of Bristol, Bristol, UK; Tyco Telecommunications, Eatontown, NJ, USA; the National Technical University of Athens, Athens, Greece; and National Telecommunications Company "Serbia Telecom," Nis, Serbia. He received B.S., M.S., and Ph.D. degrees in electrical engineering from the University of Nis, Nis, Serbia, in 1994, 1997, and 1999, respectively. His current research interests include optical networks, error control coding, constrained coding, coded modulation, turbo equalization, OFDM applications, and quantum error correction. He directs the Optical Communications Systems Laboratory (OCSL) within the ECE Department at the University of Arizona. Dr. Djordjevic serves as an Associate Editor for *Research Letters in Optics* and as an Associate Editor for *International Journal of Optics*. Dr. Djordjevic is an author of more than 90 journal publications and over 70 conference papers.

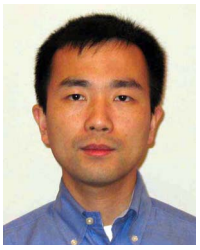

Lei Xu received the B.S. degree in geophysics from Peking University, Beijing, China, in 1997, the M.E. degree in electronic engineering from Tsinghua University, Beijing, in 2000, and the Ph.D. degree in electrical engineering from Princeton University, Princeton, NJ, in 2004. Since 2004, he has been a Research Staff Member with NEC Laboratories America, Princeton. His current research interests include advanced modulation and coding schemes for optical communications, optical signal equalization and compensation, and innovative optical devices.

Ting Wang received the M.S. degree in electrical engineering from the City University of New York and the Ph.D. degree in electrical engineering from Nanjing University of Science and Technology, Nanjing, China. Since 1991, he has been with NEC Laboratories America, Princeton, NJ, where he is currently the Department Head of optical networking research. He is the author or coauthor of approximately 70 publications and 30 U.S. patents.